Ignition Delay Correlation for a Direct Injection Diesel Engine Fuelled with Automotive Diesel and Water Diesel Emulsion

K.Alkhulaifi, M. Hamdalla

Abstract—Most of ignition delay correlations studies have been developed in a constant volume bombs which cannot capture the dynamic variation in pressure and temperature during the ignition delay as in real engines. Watson, Assanis et. al. and Hardenberg and Hase correlations have been developed based on experimental data of diesel engines. However, they showed limited predictive ability of ignition delay when compared to experimental results. The objective of the study was to investigate the dependency of ignition delay time on engine brake power. An experimental investigation of the effect of automotive diesel and water diesel emulsion fuels on ignition delay under steady state conditions of a direct injection diesel engine was conducted. A four cylinder, direct injection naturally aspirated diesel engine was used in this experiment over a wide range of engine speeds and two engine loads. The ignition delay experimental data were compared with predictions of Assanis et. al. and Watson ignition delay correlations. The results of the experimental investigation were then used to develop a new ignition delay correlation. The newly developed ignition delay correlation has shown a better agreement with the experimental data than Assanis et. al. and Watson when using automotive diesel and water diesel emulsion fuels especially at low to medium engine speeds at both loads. In addition, the second derivative of cylinder pressure which is the most widely used method in determining the start of combustion was investigated.

Keywords—gnition delay correlation, water diesel emulsion, direct injection diesel engine

I. INTRODUCTION

WATER diesel emulsion (WDE) is an alternative fuel that has been shown to reduce exhaust emissions without requiring modifications for the engine, fuel injection or exhaust systems [1-4]. The longer evaporation time of WDE along with the chemical effects of water is expected to increase ignition delay (ID) [5, 6]. The ID is the time between the start of injection (SOI) and the start of combustion (SOC). It is widely accepted that The ID has a physical and a chemical delay. The physical delay is the time required for fuel atomization, vaporization and mixing with the air, whereas the chemical delay is the pre-combustion reaction of fuel with air [7]. Ignition delay in diesel engines has a direct effect on engine efficiency, noise and exhaust emissions. A number of parameters directly affect the ID period, among them cylinder pressure and temperature, swirl ratio and misfire. In addition to these effects the recent trend of changing fuel quality and types has a great effect on ignition delay.Experimentally, the start of ignition is mainly determined by the first appearance of visible flame on a high

Correspondent author: Dr. Khalid Al-Khulaifi, email: kalkhulaif@gmail.com.Dahiat Abdulla Alsalem – Kuwait City, Kuwait

speed video recording [8], or sudden rise in cylinder pressure or temperature caused by the combustion [9].

Over the years, many correlations have been developed for predicting the ID period in diesel engines. A number of these correlations use an Arrhenius expression similar to that proposed by Wolfer [10] in 1938 where he measured the ignition delay using a constant volume bomb and expressed it as a function of pressure and temperature of the environment through the following semi-empirical equation ,

$$t_{id} = FP^{-N} \exp(\frac{E}{R_u T}) \qquad (1)$$

Where P and T are cylinder pressure and temperature respectively, E activation energy, R_u is the universal gas constant, F and N are constants. It was found that these constants vary by several orders of magnitude according to the experimental work [10-14]. Most of these ID correlations were developed from data collected in constant volume bombs [10-13] which cannot capture the dynamic variation in pressure and temperature during the ignition delay as in real engines. Based on the semi-empirical equation developed by Wolfer [10], Watson [14] developed an ID correlation using a diesel engine under steady state conditions which is still widely used;

$$t_{id} = 3.45P^{-1.02} \exp(\frac{2100}{T}) \qquad (2)$$

Later Assanis et. al. [15] developed an ignition delay correlation for predicting the delay period in a heavy-duty turbocharged direct injection diesel engine running under both steady state and transient operation. They found a functional dependence of ignition delay on equivalence ratio, pressure and temperature in the cylinder;

$$t_{id} = 2.4\phi^{-0.2}P^{-1.02} \exp(\frac{2100}{T}) \qquad (3)$$

Later they compared their new correlation against that of Watson [14] and Hardenberg and Hase [16] for steady-state conditions of a direct injection diesel engine. The later two correlations were specifically developed using diesel engine data unlike other ID correlations that were developed from measurements in combustion bombs and flow reactors [17-19]. The comparison between Assanis et. al. [15], Watson [14] and Hardenberg and Hase [16] showed that at steady state conditions only Watson [14] provided a similar degree of

accuracy as to Assanis et. al. [15] new ID correlation. Watson [14] and Assanis et. al. [15] ID correlations are based on the mean pressure and temperature. This requires the start of injection (SOI) and the start of combustion (SOC) to be known prior to the application of any of these correlations.

The goals for the work presented here are as follows:

1. To determine experimentally the ID period by conducting a series of experiments on four cylinders direct injection diesel engine running under steady state conditions fueled with automotive diesel (AD) and water diesel emulsion fuels.

2. To examine the most widely used approaches in determining the start of combustion (SOC).

3. To examine Assanis et. al. [15] and Watson [14] ID correlations against experimental data.

4. To develop an ID correlation for direct injection diesel engine under steady state operating condition based on the ID experimental data for both fuels.

II. EXPERIMENTAL SETUP

2.1 Engine setup

All tests were conducted on a four cylinder, 4.009L, Hino direct injection naturally aspirated diesel engine. The engine has a toroidal piston bowl shape and is a typical medium speed diesel engine. The fuel injection system utilizes a BOSCH A-type in-line fuel pump and a hole type injector nozzle. The injector was instrumented for needle lift providing injection-timing data. The engine was attached to an eddy-current dynamometer. All the test cell measuring devices were calibrated before the start-up of the experiment. The overall experimental setup is shown in Figure 1 while engine and injector specifications are listed in Table 1.

The standard air filter has been removed and replaced with 50L air box in order to damp out the flow pulsations in the intake manifold. This provides a steady state inlet flow condition for intake measurements. Engine coolant temperature was controlled and monitored by routing cooling water through an external heat exchanger.

2.2 Instrumentation and Data Acquisition

Three data acquisition systems were used to gather and record engine data. An engine performance data acquisition system was used to monitor and record engine load, air and fuel flow rates, relative humidity, and engine exhaust, fuel, inlet air, engine oil and coolant temperatures. The airflow rate was measured using a turbine flow meter. The intake manifold was instrumented with an absolute pressure transducer and a thermocouple. The fuel flow mass was measured using "S" beam load cell loaded in tension. The load cell output was displayed on a triple range indicator as well as the dynamometer output. Humidity and temperature sensors were placed in the engine test cell. A thermocouple was placed in the exhaust manifold near the exhaust valve to measure the exhaust temperature. Another thermocouple was also used to measure engine coolant temperature and was used as a reference to determine when the engine reaches a steady state condition. All the thermocouples used were of K-type.

The second data acquisition system was used to monitor and record cylinder pressure, needle lift and fuel injection pressure readings at each crank angle position. A piezoelectric high-pressure transducer was mounted on cylinder number one for recording cylinder pressure. The fuel pressure was measured using a fuel line high-pressure transducer. A sensor was used for monitoring the needle lift. The output of the transducers and the needle lift sensor were all fed to charge amplifiers and eventually fed to a data acquisition board. The crank angle position was measured using an optical encoder mounted on the front pulley of the crankshaft. The second data acquisition system output signals were all fed into an AVL Indimeter 619, which was used for continuous engine monitoring. The Indimeter 619 output signal was acquired using a PC with AVL Indicom software, which records and visualizes the in-cylinder data at each pulse. This gives 7200 data points for each cycle. The data produced represents an ensemble average of 30 cycles.

The third acquisition system used was an exhaust gas analyzer that measures and records NO_x (ppm), CO (%), CO_2 (%), HC (ppm) and O_2 (%).

2.3 Experimental Uncertainties

The types of errors considered in this work are bias (B_r) error and precision (P_r) error. Since all experimental results in this work were repeated three times, multiple results of a variable will lead to precision error. Uncertainty (U_r) is the combination of both bias and precision errors. As is the case for the vast majority of engineering tests, in this present work the estimate of uncertainty is made at 95% confidence level. Methodology used here in calculating experimental uncertainties can be found in details in reference [20]. The resolutions for the instruments used in this work are shown in Table 2. For each experimental result, equations that are used in engine performance or exhaust emissions calculations are determined first. Then the bias limits (sensitivity coefficients) contributing to the final result are identified and combined. Table 3 shows the overall average of uncertainties at all engine speeds and loads.Uncertainties of exhaust emissions are calculated in the same manner as engine performance. However, calculations are made at all engine speed and 200 N.m, which corresponds to the maximum expected error in the measurement than at 150 N.m. Therefore, the uncertainties at 200 N.m are used as overall average values, Table 4. Cylinder pressure readings represent an average of 10 cycles running at 1200 RPM speed and 150 N.m load. The maximum standard deviation in pressure readings between the average of these 10 cycles and their actual data is as high as 0.7 BAR, which gives high confidence in the average cylinder pressure values used in the data analysis, Figure 2. Smoothing technique of 5 points moving average is used here in order to minimize the noise in cylinder pressure readings. A comparison between this technique, 3 and 7 points moving average shows statistically a negligible difference in pressure readings among these moving average points as shown in Figure 3. The maximum deviation

value between 3 and 5 points is 0.7 BAR while the maximum deviation between 5 and 7 points is 0.5 BAR. In both cases, the maximum variation in pressure reading is 0.02 BAR. The smoothing technique has a small effect on heat release rate with a maximum standard deviation of less than 0.03 BAR, Figure 4.

2.4 Experimental Data Analysis

In order to ensure the same ambient conditions when calculating engine performance for all test points, engine brake power, fuel and air consumption calculations were corrected in accordance with SAE J1349. The eddy-current dynamometer reading was also corrected using SAE J2177. An in-house computer program was written for correcting all engine performance data in accordance with the SAE standards with 95% confidence level.

2.5 Tested Fuels

Experimental work was conducted using standard automotive diesel (AD) and water diesel emulsion (WDE). The properties of the two fuels are shown in Table 5. The WDE fuel consists of 13% volumetric fraction of water, 0.2% of 2-EHN and 2% stabilizing agent. The cetane number for WDE is the same as the AD due to the addition of 2-EHN which compensated for the cetane loss. Tests on WDE were compared later against AD fuel.

III. RESULTS AND DISCUSSION

3.1 Method used in determining the start of combustion

Selecting the proper method in determining the start of combustion (SOC) is a key issue in ignition delay studies. A number of methods are used to determine the SOC [7, 17, 21] among them is the second derivative of cylinder pressure. It was concluded by Syrimis [22] and Assanis et. al. [15] that the second derivative for determining the SOC is more reliable than any other methods.

Although the method in determining the SOC in this work is based on the change of gradient in heat release curve, its choice is examined here. The second derivative of cylinder pressure is investigated using AD experimental data as shown in Figure 5. The peak pressure of the second derivative occurs at about the sudden rise of cylinder pressure which implies the SOC point. However, looking at the heat release curve for the same test point reveals that the sudden rise of the heat release curve occurs much earlier than the crank angle at which the second derivative of cylinder pressure is a maximum, Figure 6. In the heat release curve the SOC is determined by the minimum value on the curve. From Figures 5 and 6, the cylinder pressure corresponding to the second derivative peak occurs about the midpoint of the rise of the premixed combustion period (defined by the diamond shape mark). The earlier detection of the SOC which corresponds to the rise in the HRR curve shows that this method is more sensitive to the change in cylinder pressure. This also indicates that the abrupt change in cylinder pressure is not the true location of SOC. Therefore the heat release curve is the only criterion that has been used in this work for detecting the SOC.

3.2 New Ignition Delay Correlation

It is important to show the ID experimental data for each fuel separately in order to compare predictions of Assanis et. al. [15] and Watson [14] ID correlations with the experimental data. Hardenberg and Hase [16]. ID correlation prediction values for this work were small compared to the experimental data and remains almost constant (0.25ms) throughout the engine speed range. Therefore, it will not be shown here. Experimental ignition delay data over the range of engine speeds and loads for AD are shown in Figure 7. The ignition delay period decreases as engine speed and/or load increases in accordance with Assanis et. al. [15]. This decrease can be explained due to the reduction in the physical delay, resulting from faster vaporization of fuel droplets due to higher cylinder temperature. The fast vaporization of fuel droplet is due to the increase of fuel injection pressure which decreases the fuel droplet diameter. This increase in fuel injection pressure reduces the surface area of the droplet and hence reduces the physical delay period.

[14] and [15] ignition delay predictions for both loads are shown in Figures 8 and 9. Both correlations have successfully detected the change in ignition delay for all engine speeds especially at lower load. However, [15] correlation shows better agreement with the experimental data than Watson's [14] especially at low to medium (1200- 1800 RPM) engine speed for the two loads. Correlating ignition delay with cylinder pressure and temperature using an Arrhenius expression as it is the case with both Assanis et. al. [15] and Watson [14] correlations seems to result in acceptable results compared to the experimental ID measurements. However, the difference between their predictions and experimental data should be compensated by adding and adjusting the empirical constants. As shown in the Figures 8 and 9, Assanis et. al. [15] ID correlation resulted in better predictions of ID, however, the equivalence ratio used in their correlation does not vary significantly with engine speed and/or load unlike the ID, Figure 10. Therefore, the new term to be added to the ID correlation must detect the change in engine operating conditions. A number of trials have been made during this study to find out which term must be added or adjusted to the Assanis et. al. [15] correlation to have a better agreement between predicted and experimental ID data.

Engine brake power fraction (BP) is defined in this present work as the ratio of the engine brake power at any test point to the maximum brake power of the engine. It is proposed in this work that adding BP to the ID correlation would result in a better agreement with the experimental data than using the equivalence ratio. Since engine brake power is dependent on torque and engine speed, BP is then expected to vary throughout the engine speed range and both loads unlike the equivalence ratio that was used by Assanis et. al. [15] remains almost constant throughout the engine speed range, Figure 10. Since both engine speed and load have significant effect on cylinder temperature and pressure which directly affect ID, therefore using BP is expected to result in a better prediction of ID than using the equivalence ratio.

Assanis et. al. [15] and Watson [14] used the mean values of pressure and temperature during the ignition delay for their correlations. However, for the newly developed ID correlation the values of pressure and temperature at the SOC are used. An immediate advantage of this approach is that it is not necessary to know the start of fuel injection, which makes this technique less expensive since no data acquisition system is required to detect the SOI and faster in computation time. Therefore, the new ID correlation is given by the following equation:

$$t_{id} = A(BP)^{-N} P_{SOC}^{-B} \exp\left(\frac{E}{R_u T_{SOC}}\right) \quad (ms) \qquad (4)$$

The adjustable constants (*A*, *N* and *B*) as shown in (*Eq. 4*) were fitted in order to minimize the least square error between measured and correlated ignition delay. The best-fit curve produced values for the exponentials *A*, *N* and *B* to be *2.05*, *0.4* and *1.05* respectively. Since the activation energy depends on the intensity of a molecular collision and the cetane number as proposed by Hardenberg and Hase [16], it was kept constant at the value used by Assanis et. al. [15] for the two fuels used. The resulting expression for the new ignition delay correlation is,

$$t_{id} = 2.05(BP)^{-0.4} P_{SOC}^{-1.05} \exp\left(\frac{2100}{T_{SOC}}\right)(ms) \qquad (5)$$

The new ignition delay correlation (*Eq. 3*) is compared with Assanis et. al. [15] (*Eq. 3*) and Watson [14] (*Eq. 2*) correlations using AD, Figures 11 and 12. The new correlation developed here based on the experimental ID results has successfully detected the change in ignition delay for all engine speeds at both loads. Furthermore, it appears to predict ignition delay with higher accuracy than both Assanis et. al. [15] and Watson [14] correlations for nearly all test points. In general, using the engine brake power fraction instead of the global equivalence ratio has proven to result in a better prediction of ignition delay periods for the direct injection diesel engine in use.

The new ignition delay correlation along with Assanis et. al. [15] and Watson [14] correlations are also used for predicting the delay period while operating the engine on WDE fuel. The experimental ID data over the range of engine speeds and loads for WDE is shown in Figure 13. The same trend for AD was also observed with WDE. Ignition delay for WDE also decreases as engine speed and/or load increases. However, the gradient of ignition delay data at both loads is shallow compared to AD ignition delay curves. This implies that the physical delay for WDE does not change much as engine speed or load increases. WDE for almost all of the test cases resulted in longer ID compared with AD which is consistent with previous studies [23-28]. However, other test points (1200-1600) showed a decrease in ID for WDE compared to AD. This could be as a result of having a higher cylinder temperature at the point of fuel injection which will result in shorter ID.

Figures 14 and 15 show Assanis et. al. [15], Watson [14] and the new ID correlations results for WDE. The adjustable exponentials when using WDE have been corrected to give the least square fit for the newly developed correlation.

The new adjustable constants (*A, N and B*) are *2.6*, *0.1* and *1.05* while the activation energy is held at *2100*. The ignition delay correlation now becomes,

$$t_{id} = 2.6(BP)^{-0.1} P_{SOC}^{-1.05} \exp\left(\frac{2100}{T_{SOC}}\right) \quad (ms) \qquad (6)$$

The new ignition delay correlation (*Eq. 6*) is able to predict the delay period of WDE with an acceptable accuracy compared to other correlations, particularly for the 200N.m load.

IV. CONCLUSIONS

In this study, the effect of automotive diesel and water diesel emulsion on ignition delay under steady state conditions of a direct injection diesel engine has been experimentally investigated. The investigation was carried out using four cylinders, direct injection naturally aspirated diesel engine over a wide range of engine speeds and two loads while using AD and WDE fuels for comparison reasons. The experimental data of ignition delay for automotive diesel were compared with predictions of Assanis et. al. [15] and Watson [14] ignition delay correlations. Assanis et. al. [15] correlation showed a better agreement with the experimental data than Watson's [14] especially at low to medium engine speeds at both loads. However, the deviation between Assanis et. al. [15] ID correlation and experimental data required some parameters to be added and/or adjusted. Therefore, a new correlation was developed in this study in order to have a better prediction of ignition delay for AD and WDE fuels under steady-state conditions at higher speeds and higher loads. The newly developed ignition delay correlation has shown better agreement with the experimental data than Assanis et. al. [15] and Watson [14] for both fuels at higher speeds and higher loads. The ID correlation constants may need to be adjusted according to engine type and size in order to minimize the least square error between measured and correlated ignition delay values. In addition, the second derivative of cylinder pressure which is the most widely used method in determining the start of combustion was investigated. The sudden change of gradient in heat release curve showed to be more reliable in detecting the SOC than the second derivative of cylinder pressure method.

REFERENCES

[1] Brown, K.F., D.D. Chadderton, and D.D. Lnger, Opportunity for diesel emission reductions using advanced catalysts and water blend fuels. SAE 2000-01-0182, 2000.

[2] Daly, D.T. Future fuels and fuel additives for vehicle emissions control. 2000. San Francisco, CA: American Chemical Society National Meeting.

[3] Daly, D.T. and D.A. Langer. Low emission water blend diesel fuel. 1999. Toronto, Canada: Canadian Mining Diesel Conference Proceedings.

[4] Subramanian, K.A. and A. Ramesh, Use of Hydrogen Peroxide to Improve the Performance and Reduce Emissions of a CI Engine Fuelled with Water Diesel Emulsions. 2008.

[5] Greeves, G., I.M. Onion, and G. Khan. Effects of water introduction on diesel engine combustion and emissions. in 16th symposium international on combustion. 1976: The Combustion Institute.

[6] Radwan, M.S. and H. Salem, A study of some combustion characteristics of gas oil/water emulsions in a swirl chamber diesel engine. SAE 892056, 1989.

[7] Heywood, J.B., Internal combustion engine fundamentals. 1988.

[8] Lee, J.H. and N. Lida, Combustion of diesel spray injected into reacting atmosphere of propane-air homogeneous mixture. Int. J. Engine Res., 2001. 2(1): p. 69-80.

[9] Aligrot, C., J.C. Champoussin, N. Guerrassi, et al., A correlative model to predict autoignition delay of diesel fuels. SAE transactions, 1997. 106(3): p. 958-963.

[10] Wolfer, H.H., Ignition lag in diesel engines. VDI-Forschungsheft, 1938. 392: p. 621-436.047.

[11] Hiroyasu, H., T. Kadota, and M. Arai, Development and Use of a Spray Combustion Modeling to Predict Diesel Engine Efficiency and Pollutant Emissions: Part 2 Computational Procedure and Parametric Study. Bulletin of JSME, 1983. 26(214): p. 576-583.

[12] Kadota, T., H. Hiroyasu, and H. Oya, Spontaneous ignition delay of a fuel droplet in high pressure and high temperature gaseous environments. JSME, Bulletin, 1976. 19: p. 437-445.

[13] Stringer, E.W., A.E. Clarke, and J.S. Clarke, The spontaneous ignition of hydrocarbon fuels in a flowing system. Proc. Inst. Mech. Eng, 1970. 184: p. 212–224.

[14] Watson, N., A.D. Pilley, and M. Marzouk, A Combustion Correlation for Diesel Engine Simulation. SAE 800029, 1980.

[15] Assanis, D.N., Z.S. Filipi, S.B. Fiveland, et al., A predictive ignition delay correlation under steady-state and transient operation of a direct injection diesel engine. J. Eng. Gas Turbines Power 2003. 125: p. 450.

[16] Hardenberg, H.O. and F.W. Hase, Empirical Formula for Computing the Pressure Rise Delay of a Fuel From its Cetane Number and From the Relevant Parameters of Direct-Injection Diesel Engines. SAE 790493, 1979: p. 88.

[17] Lyn, W.T. Study of burning rate and nature of combustion in diesel engines. in Ninth international symposium on combustion. 1963: The combustion institute.

[18] Spadaccini, L.J., Autoignition Characteristics of Hydrocarbon Fuels at Elevated Temperatures and Pressures. J Eng Power Trans ASME, 1977. 99: p. 83–87.

[19] Spadaccini, L.J. and J.A. TeVelde, Auto-ignition Characteristics of Aircraft-Type Fuel. Combustion and Flame, 1982. 46: p. 283-300.

[20] Stern, F., M. Muste, M.L. Beninati, et al., Summary of Experimental Uncertainty Assessment Methodology with Example. IIHR Report, 1999. 406.

[21] Henein, N.A. and J.A. Bolt, Correlation of air charge temperature and ignition delay for several fuels in a diesel engine. SAE 690252, 1969.

[22] Syrimis, M., K. Shigahara, and D.N. Assanis, Correlation between knock intensity and heat transfer under light and heavy knock conditions in a spark ignition engine. SAE 960495, 1996.

[23] Gong, J.-S. and W.-B. Fu, A study on the effect of more volatile fuel on evaporation and ignition for emulsified oil. Fuel, 2001. 80: p. 437-445.

[24] Kumar, I.N.N., S.C. Prasad, and B.V.A. Rao, Heat release rate analysis of a DI diesel engine using diesel and seawater semi-stable emulsion. SAE 2002-01-2719, 2002.

[25] Nazha, M.A.A., H. Rajakaruna, and S.A. Wagstaff, The use of emulsion, water induction and EGR for controlling diesel engine emissions. SAE 2001-01-1941, 2001.

[26] Park, J.W., K.Y. Huh, and J.H. Lee, Reduction of NOx, smoke and BSFC with optimal injection timing and emulsion ratio of water-emulsified diesel. Inst. of Mech. Engr., 2001. 215(D): p. 83-93.

[27] Tajima, H., K. TAKASAKI, M. Nakashima, et al. Visual study on combustion of low grade fuel water emulsion. in COMODIA. 2001. Nagoya, Japan.

[28] Wang, C.-H. and J.-T. Chen, An experimental investigation of the burning characteristics of water oil emulsions. Heat Mass Transfer, 1996. 23(6): p. 823-834

TABLE I
TEST ENGINE SPECIFICATIONS

Bore (B) x Stroke (l)	104 x 118(mm)
Compression Ratio (r)	17.9
Connecting rod length (L)	181.75 (mm)
Injector Nozzle (D_n)	5 holes x 0.29 mm dia x 160 deg cone angle
Needle opening pressure	215BAR
Valve timing	IVO (8^0 BTDC) – IVC (48^0 ABDC) EVO (60^0 BBDC) – EVC (8^0 ATDC)
Fuel pump plunger	9.5 mm dia x 8 mm max. stroke
Piston bowl shape	Toroidal

TABLE II
RESOLUTION OF EXPERIMENTAL INSTRUMENTS

Instrument	Resolution
Crank angle encoder	+/- 0.1^0
Pressure Transducer	+/- 0.3%
Inlet air mass	+/- 1%
Inlet fuel mass	+/- 0.2%
Humidity	+/- 4%
Thermocouples	+/- 0.3^0C
Dynamometer Indicator	+/- 0.01%
CODA (Exhaust emissions) **HC** **CO** **CO$_2$** **O$_2$** **NO**	 +/- 4ppm +/- 0.02% +/- 0.3% +/- 0.1% +/- 25ppm

TABLE III
OVERALL AVERAGE UNCERTAINTIES (+/-) FOR ALL ENGINE TEST POINTS

Measurement	Average Uncertainty (abs.)	Average Uncertainty (%)
RPM	1.00	0.06
Torque(N.m)	1.09	0.61
Exhaust temperature(^{0}C)	2.41	0.58
Inlet air temperature(^{0}C)	0.37	1.67
Humidity(%)	0.41	0.41
Fuel mass(g)	2.82	1.88
Air mass flow rate(g/s)	0.11	0.20
Time(s)	0.13	0.15
Fuel mass flow rate(g/s)	0.04	1.81
Air mass(g)	0.05	0.07
Volumetric efficiency(%)	0.17	0.17
Brake power(kW)	0.21	0.61
BSFC(g/kW.h)	4.47	2.04

TABLE IV
OVERALL AVERAGE UNCERTAINTIES (+/-) IN EXHAUST EMISSION INDEX

Emission Index ($g_{species}/g_{fuel}$)	Average Uncertainty (abs.)	Average Uncertainty (%)
CO_2	0.0019	2.44
HC	0.0019	4.12
O_2	0.0753	2.36
NO_x	0.0014	3.91

TABLE V
SPECIFICATIONS OF THE TEST FUELS

Properties	AD	WDE
Density @ 15 ^{0}C, kg/m^3	839	876.7
Viscosity @ 40 ^{0}C, m^2/s	3 x 10^{-6}	3.27 x 10^{-6}
Flash point ^{0}C	67	65.6
Distillation (^{0}C) Initial boiling temp. T 10% T 50% T 90% Final boiling temp.	182 216 272 338 358	
Boiling temp. ^{0}C, (initial)	184	97.8
Auto ignition temp. ^{0}C	254 - 285	>250
Sulphur, ppm	462	<5000
Cetane Number	51.5	Min 51
Water, %vol. (mass %)	-	13 (14.8)
Diesel Fuel, %vol. (mass %)	100	84.4 (81.2)
Surfactant, %vol.	-	2
2-EHN, %vol.	-	0.2
Ash, %mass	<0.01	<0.01
LHV, MJ/kg	42.5	37.5
C (%), by mass	86.4	76.7
H (%), by mass	12.8	12.6
N (%), by mass	<0.05	<0.05
Color	Clear Yellow-brown	Milky white
Stoichiometric (A/F) ratio	14.35	12.3
Molecular weight (kg/kmol)	165	142

TABLE VI
ERROR PERCENTAGE BETWEEN WATSON, ASSANIS AND NEW ID CORRELATIONS RELATIVE TO EXPERIMENTAL DATA AT ALL ENGINE SPEEDS AND BOTH LOADS

RPM	Load (N.m)	Watson	Assanis	New
1200	150	-18.28%	0.16%	3.39%
1400		-27.80%	-7.59%	1.61%
1600		-34.23%	-13.87%	0.89%
1800		-46.50%	-23.75%	-4.45%
2000		-59.46%	-34.46%	-9.65%
2200		-56.32%	-31.55%	-4.73%
RPM	Load (N.m)	Watson	Assanis	New
1200	200	-21.14%	3.61%	11.82%
1400		-34.94%	-6.42%	7.78%
1600		-58.97%	-26.87%	-3.07%
1800		-64.83%	-31.64%	-4.41%
2000		-145.92%	-95.88%	-53.17%
2200		-189.60%	-131.15%	-74.57%
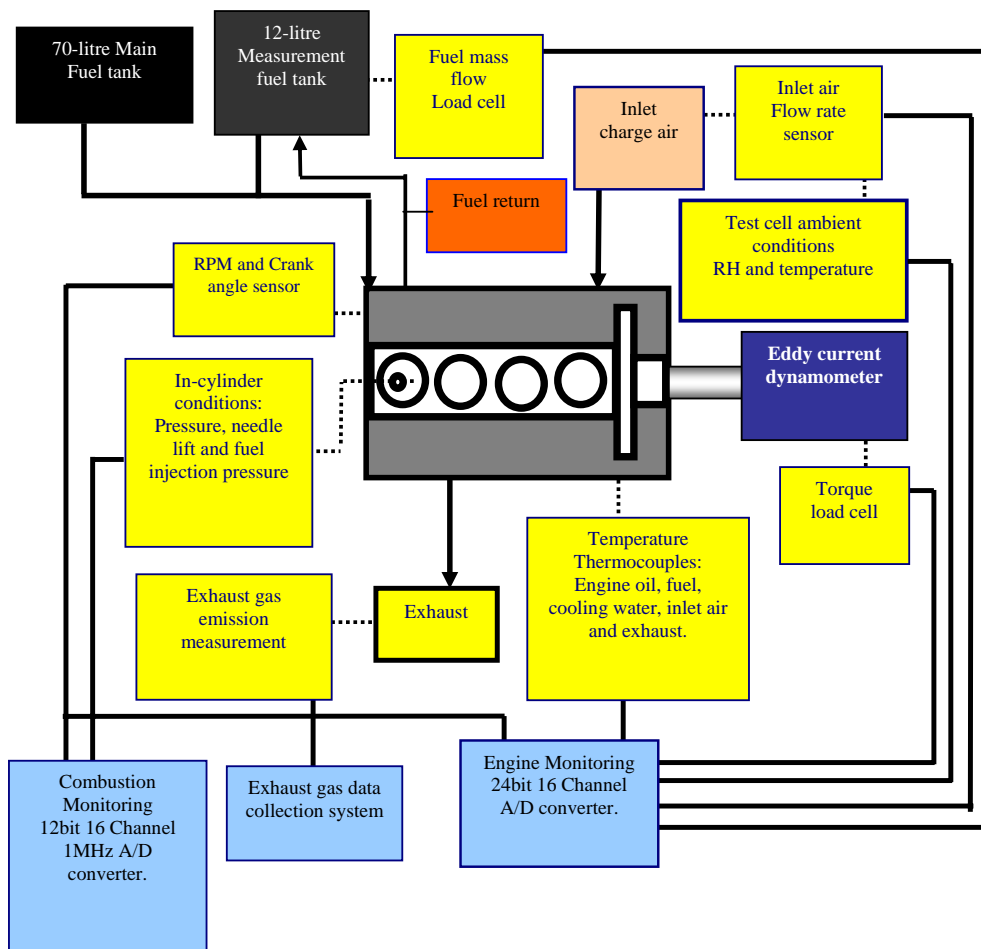
Fig. 1 Experimental setup
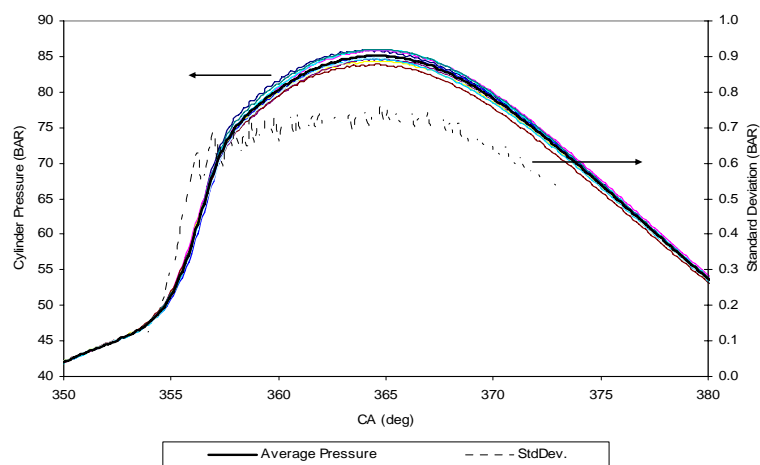
Fig. 2 Cylinder pressure curves of 10 cycles and their standard deviation at 1200 RPM and 150 N.m using AD
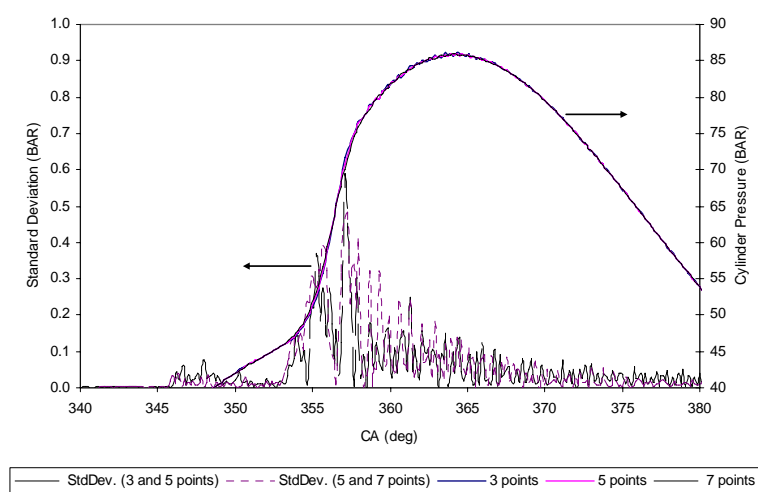
Fig. 3 Smoothing technique effect of 3, 5 and 7 points moving average on cylinder pressure curve with their standard deviation at 1200 RPM and 150 N.m using AD
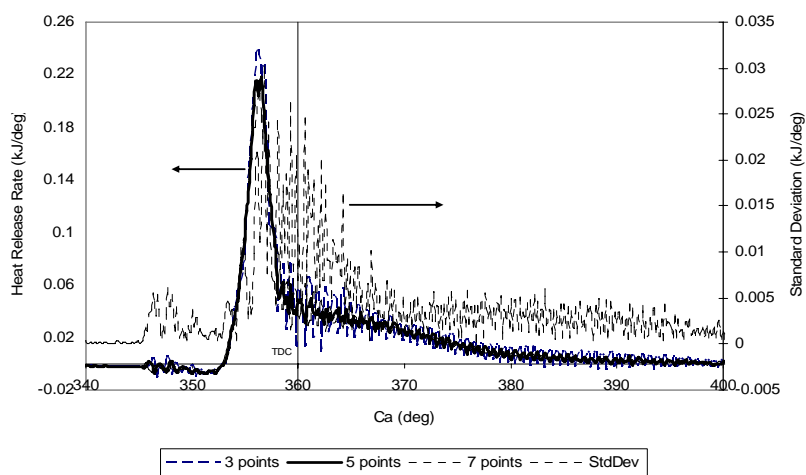
Fig. 4 Smoothing technique effect of 3, 5 and 7 points moving average on heat release rate with their standard deviation at 1200 RPM and 150 N.m using AD
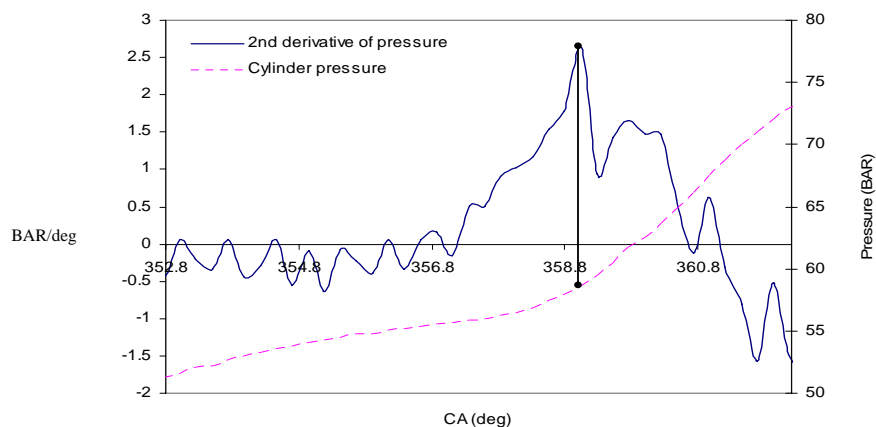
Fig. 5 The second derivative of the cylinder pressure and its coincidence with the rise of cylinder pressure at 2000 RPM and 150 N.m using AD
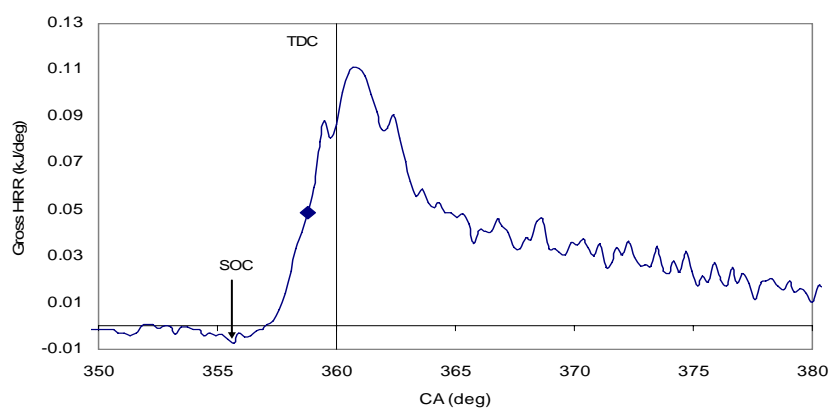
Fig. 6 HRR at 2000 RPM 150 N.m using AD where the diamond symbol shows the location of d^2P/deg^2 peak
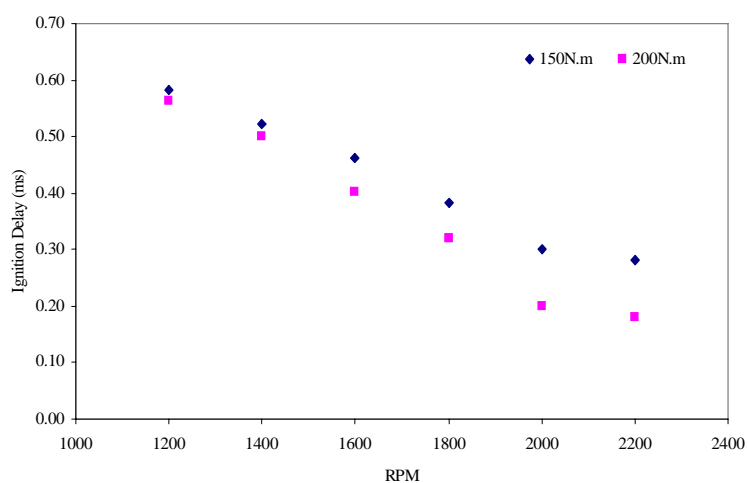
Fig. 7 Experimental ID data at steady state operation at all engine speeds and loads using AD
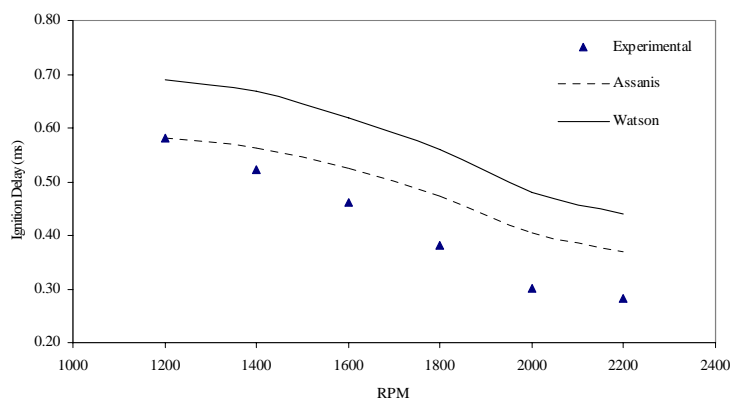
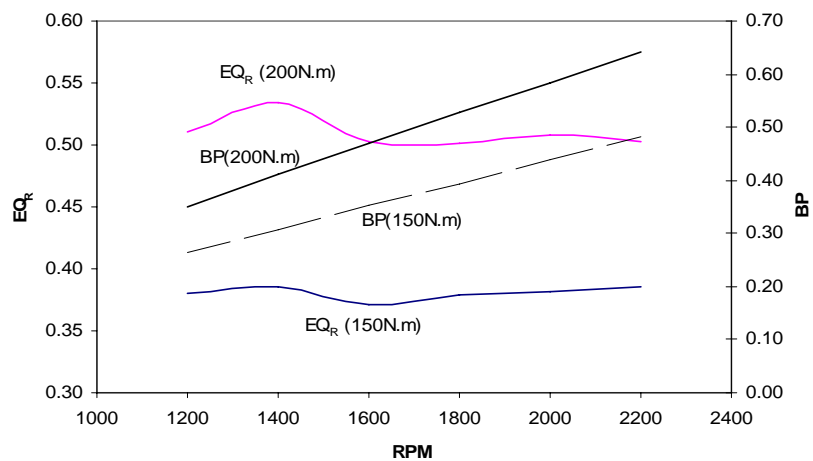Fig. 8 Comparison of Watson [14] and Assanis et. al. [15] ID predictions against experimental ID data at all engine speeds using AD at 150 N.m
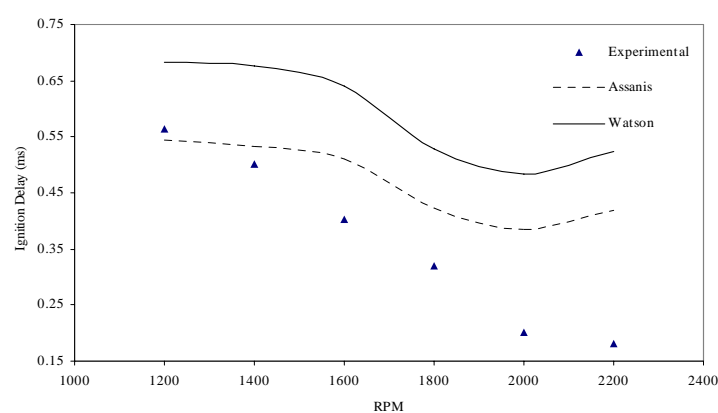
Fig. 9 Comparison of Watson [14] and Assanis et. al. [15] ID predictions against experimental ID data at all engine speeds using AD at 200 N.m

Fig. 9 Equivalence ratio and brake power fraction at all engine speeds and both loads using AD
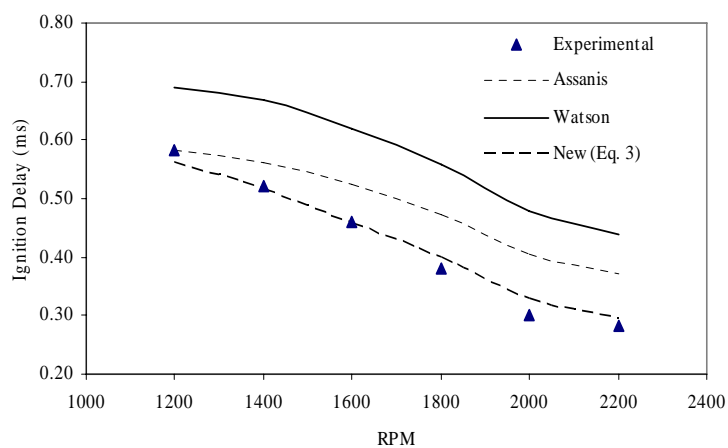
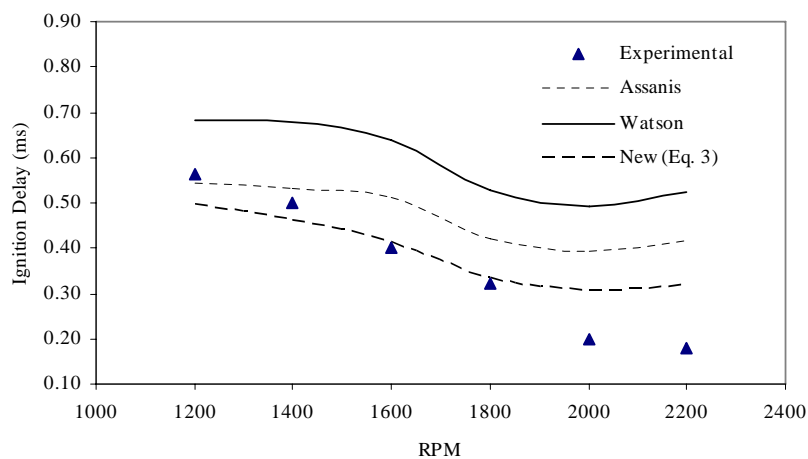Fig. 11 Comparison of different ID correlations at all engine speeds under steady state operation using AD at 150 N.m

Fig. 12 Comparison of different ID correlations at all engine speeds under steady state operation using AD at 200 N.m
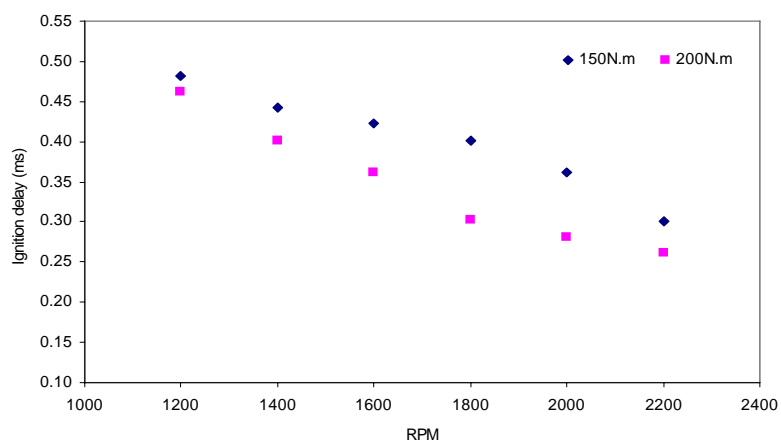
Fig. 13 Experimental ID data at steady state operation at all engine speeds and both loads using WDE
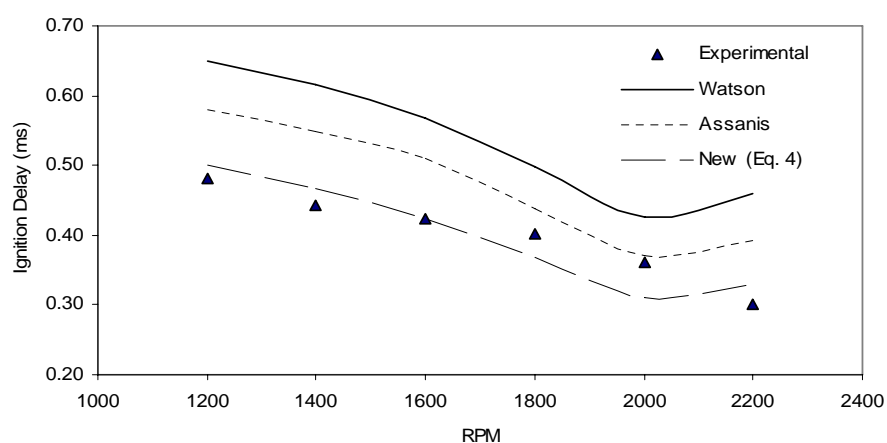
Fig. 14 Comparison of different ID correlations at all engine speeds at steady state operation using WDE at 150 N.m
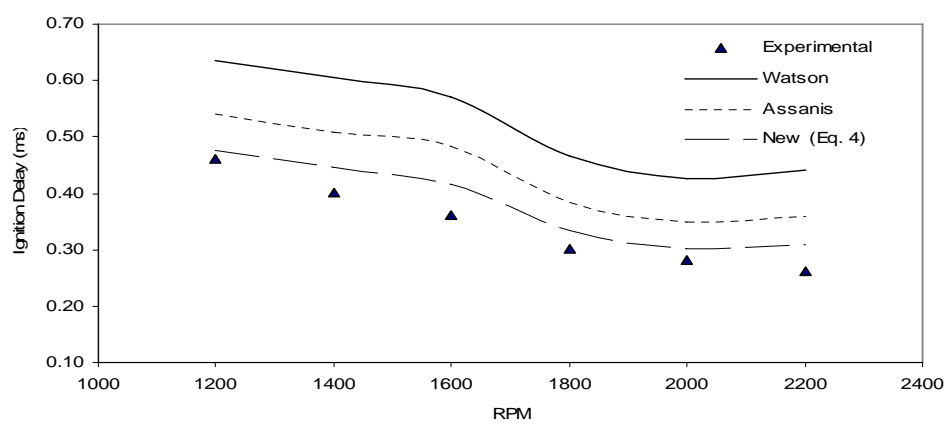

Fig. 15 Comparison of different ID correlations at all engine speeds at steady state operation using WDE at 200 N.m